Technical Report No. 15-69-MET 7

INTERACTION OF CRACKS WITH MICROSTRUCTURE IN POLYCRYSTALLINE CERAMICS

Final Report, NASA Grant NGR 18-001-038

by

MARTIN H. LEIPOLD

Department of Metallurgical Engineering

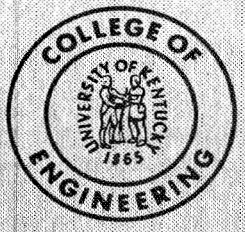

OFFICE OF RESEARCH AND ENGINEERING SERVICES

COLLEGE OF ENGINEERING
UNIVERSITY OF KENTUCKY

INTERACTION OF CRACKS WITH MICROSTRUCTURE IN POLYCRYSTALLINE CERAMICS

by

Martin H. Leipold

Associate Professor of Materials Science
Department of Metallurgical Engineering and Materials Science

* * * * * * * * *

This report is submitted as the final report of Research Grant NGR 18-001-038 from the National Aeronautics and Space Administration, whose support of the work reported is hereby acknowledged.

* * * * * * * * *

TABLE OF CONTENTS

LIST OF FIGURES

LIST OF TABLES

ABSTRACT

A technique has been developed by which a crack may be propagated in a controlled manner through a ceramic specimen, with simultaneous observation of the path of the crack and the force changes occurring during propagation. The technique requires grain sizes of the same order as the thickness of the specimen in order to separate the microstructure features influencing the crack path. Crack behavior may be observed by means of optical microscopy and would be suitable for scanning electron microscopy. Transmission electron microscopy might also be used.

Application of the technique to MgO bicrystals demonstrates the existence of strong pinning points within the individual crystals as well as at the grain boundary. The magnitude of the pinning at the grain boundary does not appear to be explainable on the basis of change of direction alone. In polycrystalline materials, this start-stop process is repeated numerous times.

INTRODUCTION

Ceramic materials, regardless of their primary application, consistently fail in service by mechanical fracture. For this reason, a great deal of research has been directed towards understanding the mechanism of this fracture.[1-4]* Much is known concerning the behavior of dislocations in ceramics and the importance of these dislocations in the process of ultimate fractures is beginning to be understood[5,6]. It has been clearly shown that dislocations may nucleate cracks in a manner which can be predicted[7]. However, once cracks exist in a polycrystalline ceramic, either as a result of this process or some other mechansim, there is little knowledge of the path and process by which this crack proceeds through the ceramic material. It is known, for example, that very fine grain ceramics tend to fracture intergranularly, while coarser grain ceramics fracture intragranularly. This transition has been shown rather clearly in recent work[8], but, of course, the transition would be expected to be influenced by impurity levels and distribution, as well as by crystallographic orientation. In spite of this importance of the detailed path of a crack moving through a ceramic, only rarely has the literature shown attempts to investigate this process on a microscopic scale[9]. Indeed, fracture studies often are based on continuum concepts, where the first assumption is that the material under study is an isotropic, homogeneous medium.

---

*Numbers in parentheses refer to the References.

Investigations of surface energies that are determined during fracture of ceramics also provide indications of the importance of the microstructure. Magnesium oxide, for example, shows up to an order of magnitude increase in apparent surface energy for polycrystals, as compared to [100] cleavage in single crystals . Many suggestions are available to explain this difference, but with no clear separation as to which, if any, of the suggestions might be primary.[10]

The objective of this research was to attempt to fulfill the need for a technique by which the motion of a crack through a polycrystalline ceramic could be studied in detail, observing the detailed path of the crack and the microstructure affecting this path, and the changes in stress accompanying this motion. The intent was to make such observations on a scale from hundreds of angstroms to mm range. Because one particular microstructural feature, grain boundary regions, was expected to be of vital importance in the mechanism, variations in the composition of this grain boundary region were attempted by means of variations in impurity level.

CRACK PROPAGATION DEVICE

The system that is used to control the propagation of a crack through a ceramic body in a scientifically useful manner must exhibit the following features:

1. small size
2. high degree of stiffness
3. capability of very small strains.

In the initial trials, two different concept approaches were used. The first employed the expansion of a reference body to place a strain on the polystalline ceramic under tests, while the second used the deformation developed in a piezoelectric crystal under an applied electric field. Both of these techniques have shown some success and are depicted schematically in Figs. 1 and 2. However, some difficulty was encountered with the piezelectric type, apparently as a result of the large number of joints required to develop sufficient deformation. These joints introduced two problems:

1. deformation that reduced the strain applied to the test ceramic
2. frequent failure in the joint, requiring reassembly of the entire device.

For these reasons, emphasis has been placed on the thermal-expansion type of unit.

A variety of configurations and forms, using the thermal-expansion principle shown in Fig. 1, were employed before the configuration shown in Fig. 3 was finally selected. The initial reason for placing the arms at a slight angle to the body of the strain device were:

1. observation of the specimen in transmitted light during testing
2. reduction of the stress at the crack tip as the crack progated.

However, early trials showed that the flexing was not sufficient to promptly control crack motion, through reduction of stress especially in the bicrystals. Once a crack began to move, it usually would continue to do so until complete failure occurred. Consequently, larger specimens were employed, extending

beyond the support arms (see Fig. 3). Thus, the technique becomes a modification of the double-beam cantilever configuration.[11] A small amount of offset remained in the arms to permit back lighting of the specimen under test.

The assembly and construction of the fracture propagation devices required utmost care to prevent electrical leaks which would destroy the output signal from the quartz tranducers. The quartz elements were silvered with Dupont #7095 silver paste. The basic assembly methods for the device employed conventional soldering techniques; however, every attempt was made to minimize the thickness of the solder joints, to reduce mechanical compliance. After the assembly was complete, the entire unit was ultrasonically cleaned in benzene and a layer of RTV 615A silicone rubber was painted over the quartz transducer. Even with these precautions, some susceptibility to atmospheric moisture remained. This usually took the form of a dc drift in the output of the transducer, even under conditions of no specimen and no thermal expansion in the device. Because of this drift, time-constants greater than 5 to 10 seconds could not be used. Since this is not an inherent shortcoming of a quartz piezelectric transducer, better results should be obtained with better controlled preparation and testing environments.

The electrical signal from the quartz transducer was fed a Kistler Model 503 charge amplifier, which was used to provide the high input impedance required for a piezoelectric element, as well as to provide some variation in electrical amplification and electrical time-constants. The time-constants that were available are shown in Table I.

TABLE I

Time-constants Available for Fracture Studies

Amplifier range setting*	Time-constants (sec.)
10	.1, 10, 10^4
5	.05, 5, 5 x 10^3
2	.02, 2, 2 x 10^3
1	.01, 1, 1 x 10^3

*Corresponds to pounds/5-volt signal.

The electrical signal is fed to a recorder of a type consistent with the frequency response desired. A Sargent Model SR-1 recorder (time constant >1 Hz), a Beck-Lee electrocardiogram recorder (time constant>30 Hz) and a Tektronix Model 564 recording oscilloscope (time constant $>10^6$ Hz) were used in these experiments.

In all cases, extensive electrical shielding was required to reduce ac pickup ahead of the charge amplifier. Double-shielded cable on the leads and a grounded-metal shield surrounding the crack propagation device on the microscope stand reduced the ac pick-up to 10-20 mV (rms).

Calibration Procedures

Several variables need to be calibrated for use in conducting a mechanical test of this type; stress, strain, and strain rate are typical. The stress calibration was conducted in the following manner. Wires were epoxy-cemented to each of the test devices so that the loads were applied in a direction parallel to that applied to the ceramic crystal. With the transducer suspended from one wire, a standard weight was repeatedly loaded and unloaded to the other wire, to provide a load-to-volts signal for each device. Although variations from device to device existed (by a factor of about 5), repeat calibrations on a given transducer over a period of time were only 5%. The sign of the calibration value was + or -, depending upon the orientation of the quartz crystal.

The strain in each device was calibrated by observing in a completely cracked specimen the change in crack size as a function of temperature. This procedure, in reality, measured the thermal expansion

of the reference body of the device, in this case, copper. The thermal expansion determined by this method averaged 10.3×10^{-6} per ^{o}F, compared to an accepted value of 9.8×10^{-6} per ^{o}F. However, because the specimen that was used for these calculations had been cracked completely through, a no-load strain actually was measured. If this amount of strain were actually applied to the ceramic specimen, stresses somewhat higher than reasonable values would have existed. Consequently, a portion of the observed strain must have occured in the testing device, probably in the joints. No satisfactory method was found for independently determining the strain under load.

The no-load strain rate could readily be calibrated by means of time-temperature heating rate curves of the crack propagation devices and the thermal expansion of the components. However, these determinations were limited to the same no-load conditions, as were the actual strain determinations.

MATERIALS

A variety of types of manganese oxide were selected for investigation as a part of the program. These types are listed in Table II. All samples were refired to $1650^{o}C$ in air for 24 hours, to obtain equilibrium conditions in terms of stress and impurity distribution. After this anneal, both of the K-type specimens had undergone bloating and did not appear as suitable for further study as the other types. Consequently, the emphasis in the testing has been placed on the JP, JF, and N materials. Typical micrographs of the JP and JF materials are shown in Fig. 4.

TABLE II

MgO Materials for Studies of
Crack Interaction with Grain Boundaries

Type	SiO_2*	CaO*	Source
JP (High purity)	100	50	Ref. 12
JF (Fisher)	1000	1000	Ref. 12
KK	300	500	Ref. 13
KJ	500	1700	Ref. 13
N^+	25	30	Norton polycrystals & bicrystals

*Supplier analysis

+Norton Research Corp (Canada) Ltd., Chippawa, Ontario.

SPECIMEN PREPARATION PROCEDURES

After annealing, specimen slabs for fracture testing were prepared using conventional geological and semiconductor machining equipment. Slabs approximately 6-10 mm on a side by a 1 mm thick were sliced from the bulk pieces of material. (In the case specimens which had been available in the form of 2 cm diameter rods, specimens took the form of quarter circles 1 mm thick). These slabs were mounted onto glass slides by means of Lakeside cement, and polished using progressively finer diamond-faced disks, and finally with 0.3 μ alumina to produce a normal metallographic finish. The specimens were then reversed on the slides, ground to 0.1 to 0.15 mm thickness and polished on the second surface. After using alcohol to free the slabs from the glass slides, they were then attached to the crack propagation devices by means of an epoxy cement and allowed to cure overnight at room temperature. A precrack was introduced into each specimen between the arms of the crack propagation device by means of a razor-blade and small mallet. The crack was extended to the center line between the attachment points of the crystal. (With bicrystal specimens, the precrack occasionally extended all the way to the grain boundary, and destroyed the value of the specimen.) The crack propagation device, with its specimen attached, was then connected to the electronic readout and power supply and placed under a stereoscopic microscope, so that the condition and progress of the crack could be observed during propagation.

Finally, power was applied at a fixed rate to the heater in the device and the recording began. Time-to-failure was normally less than one minute. In many cases where high-speed records were being made using the oscilloscope, it was necessary to delay triggering of the oscilloscope until after heating of the device had begun in an attempt to have the fracture occur during the sweep time. This was not always successful, and in some cases, failure occurred before the record was begun or during the retrace of the sweep signal. After fracture, the specimens could be demounted from the crack propagation device by softening the epoxy with a soldering iron and lifting the test specimen free. Thus, it could be retained for further study.

With the bicrystals, some knowledge of the crystallographic directions was necessary. This was normally determined by cleavage behavior and birefringence induced by stress. The grain-boundary tilt angle was determined by measurement, with one crack plane vertical. The twist angle was estimated from the thickness of the crystal and the amount of exposed cleavage face.

It was originally planned to use the transmissional electron microscope as well as the optical microscope to observe conditions surrounding the tip of a crack under dynamic conditions. However, after substantial effort at preparing suitable specimens by chemical or mechanical techniques, the effort was abandoned. Only ion-bombardment thinning would appear capable of producing the relatively large area and relatively uniform thinness required for this test. Access to this type of preparation equipment is not presently available.

RESULTS

Application of this crack propagation device, using different types of MgO produced both qualitative and quantitative results. Since these differ somewhat for each material, they will be discussed in turn, first describing the qualitative results, i.e. , the form in which the failure proceeded, and secondly, where possible, the quantitative results obtained.

Glass Cover Slips

The samples, although not described in detail under materials and were used primarily as evaluation material, were a conventional soda-lime-silicate glass, 0.1 mm thick. Pieces were cut and, with the exception of an alcohol rinse, were used as obtained.

The propagation of cracks through these glass cover slips was a slow, easily controlled process. The crack could easily be started and stopped, and crack running speeds of the order of 0.1 mm/sec were normally obtained. The cracks normally slowed down and stopped as they approached the edge of the specimen. Consequently, little elastic energy remained in the specimen at the conclusion of the test. The cracks were generally perpendicular to the direction of loading and proceeded along a straight path. An example of an after-cracked specimen is shown in Fig. 5.

Attempts to determine the surface energy from the fracture dynamics were frustrated by two factors. First, recent work has clearly demonstrated that the available analysis of surface energy from

fracture behavior does not apply to this specimen configuration because of insufficient ratio of crack length to arm width.[14] This same shortcoming, unfortunately, presently prevents analysis of surface energy in the MgO bicrystals as well. It is possible that a mathematical analysis of this configuration will become available. The second problem in the calculation of surface energies with this system and the glass samples results from the time-constant of the systems. The stress signals accompanying the slowly propagating cracks in glass have a time-constant greater than those usable in the system because of drift. Consequently, the force output signals from the glass samples showed substantially no output, since the rate of signal generation was considerable less than the rate of signal delay. This is not a fundamental limitation, since the time-constant of the testing devices could be increased to perhaps hundreds or thousands of seconds, if better conditions were available for preparation and encapsulation of the crack propagation devices.

Since glass, of course, exhibits no microstructure, no investigations of its influence on crack behavior could be made. Further tests and analysis were not attempted.

Norton Bicrystals

The bicrystal samples were the most applicable to this type of testing, since the grain diameters are clearly greater than the thickness of the specimen. Crack propagation within each of the grains in these

bicrystals (that are remote from the boundary) took two forms: conventional cleavage on the [100] plane and fracture on non-[100] planes. The latter occurred only rarely and for short distances. It took the form of a very show, irregular tearing type of fracture, which, to the limit of optional resolution, did not consist of alternate [100] fractures. Crack speeds here were of the order of 0.1 mm per second. With [100] cleavage, slow growth was noted in some cases, but in most, cracks would be locked motionless. When the crack broke loose it would travel at very high speeds, with a substantial release of energy. The details of the locking process are not completely clear. In many cases, of course, grain boundaries provided this lock, as will be discussed later. However, in some cases, cracks were stopped in the interior of the grain. Although precipitates are likely mechanisms for such locking, none were evident with the resolution available here (about 5 μ).

Examples of the different types of fracture behavior observed with the Norton bicrystals are shown in Figs. 6 thru 9. The first of these (Fig. 6) shows crack locking within the grain, and a complex fracture once propagation has begun. During the test, the crack remained locked at the end of the precrack, by some mechanism, until a calculated deflection of 8×10^{-3} mm had been placed on the crystal. At this point, the crack proceeded along the complex path shown. With the recording speed used in this test, the crack velocity was too high to permit observation of additional changes in stress either at the intersection with the grain boundary or the change from non-[100] to [100] fracture.

Two factors, however, are evident:

1. Cracks are locked by some feature within the grain to an extent at least as great as that introduced by the grain boundary. In this case, subsequent re-examination at the point where the precrack had stopped revealed no observable microstructure. However, higher resolution may have been required. (The initial locking of the crack is not an inherent mechanism, as, for example, atmospheric blunting , since many [100] cleavages proceed slowly and controllably upon the application of stress.)

2. The second observation is that fracture does not always proceed along [100] planes in MgO and, consequently, attempts to evaluate polycrystalline fracture energies must include some cleavage energy as a result of non-[100] fracture.

Figure 7 provides another type of observed behavior. Here, the crack proceeded slowly from the precrack to point 1 and then remained locked while stress increased. After 1×10^{-3} mm of additional strain the crack proceeded quickly to point 2 along a new direction. This temporary pinning may have beem similar to that observed in Fig. 6 or it may have been influenced by the crack beginning to proceed over the epoxy cement. At the grain boundary, point 2, the crack remained locked until a calculated strain of 20×10^{-3} mm was introduced. At this point, the fracture proceeded to failure, with a recorded force reduction of 2.7 lbs. This force is not entirely from fracture energy since the crack proceeded completely out of the crystal upon failure, and therefore includes an unknown amount of kinetic energy.

Figure 8 shows an example of a fracture which extended slowly from the crack to the grain boundary, where it remained fixed until an additional 5×10^{-3} mm of strain was introduced. The crack then proceeded with high velocity out of the boundary to failure. Figure 9, in contrast, shows a crack which was locked briefly at the end of the precrack, then proceeded to the boundary, through the boundary, and out the other side, with no discernable hesitation at the grain boundary. The change in angles at the boundary in Figs. 8 and 9 are very similar, and should exhibit comparable increases in stress for repropagation. Since they do not, it is suggested that the mechanism of crack interaction with grain boundaries is more complicated than that suggested by Gell and Smith[15], at least in this material.

Polycrystals

Although a large variety of types of polycrystalline ceramic materials was planned for testing, data were actually obtained from only three of these. As mentioned above, the K-type materials were not tested further after reheating. The JF and JP specimens did not undergo sufficient grain growth during reheat to produce a large enough grain size to permit preparation of samples with average grain diameters greater than thickness. However, tests were made and will be discussed. One sample of N-type fused material, which, in reality, was polycrystalline in nature (grains $>.1$ mm in diameter) was received and would have been ideal for study. However, the quality of the grain boundaries was

so poor that either the slabs came apart during preparation and handling or the specimens failed during the first application of load.

The results obtained on the JP material are shown in Table III. Many tests were conducted and all showed very similar behavior. The process of crack motion was quite slow, with the crack easily being stopped and started if desired. Propagation rates were of the order of 0.1 mm/sec. This is an average rate based on total time to failure and not instantaneous rates. The repeated start-stop process clearly shows the number of times a crack stops and is reinitiated by the stress.

Attempts were made to associate the stress increase before propagation with stress change during propagation, and the number of start-stops with grain size. However, neither correlation was obtained, as may be concluded from Fig. 10 & 11. Approximating the distance traversed by each propagation from the velocity and the time between propagations, values ranging from 15 μ or less to 300 μ are obtained, as compared with a relatively uniform grain size near 75 μ.

Because of the somewhat smaller grain size of these specimens, it was not possible to differentiate the particular microstructure features resulting in the crack stoppage. Larger grain sizes should have been obtainable with higher temperature treatment. However, facilities were not available to obtain this additional grain size.

The JF material showed results quite similar to those from the JP material. The testing conditions, parameters, etc., are very similar to those shown in Table III. Likewise, the average crack

TABLE III

Fracture Conditions for JP Polycrystalline Material

Sample	Thickness (μ)	Time-constant (sec)	*Pull rate (mm/sec)	Average crack vel. (mm/sec.)
XIV 4	140	.05	4.5×10^{-4}	.1
XIV 6	80	.05	4.5×10^{-4}	0.03
XV 2	100	2	4.5×10^{-4}	0.07
XV 3	110	.05	4.5×10^{-4}	0.03
XV 4	130	5	4.5×10^{-4}	0.08
XV 5	150	5	4.5×10^{-4}	0.09
XV 6	130	.05	4.5×10^{-4}	0.11
XVI 1	85	.05	4.5×10^{-4}	N.A.+
XVI 2	155	.05	4.5×10^{-4}	N.A.
XVI 3	140	.05	4.5×10^{-4}	N.A.
XVI 4	65	.05	4.5×10^{-4}	N.A.
XVI 5	75	.05	4.5×10^{-4}	N.A.
XVI 6	75	.05	4.5×10^{-4}	N.A.

+N.A. - Not Available

*Calculated rate of separation of loading arms on "Gilman" specimen.

velocities were within an identical range. The only difference is typified in Fig. 12. The scale of the start-stop process is finer on the average than with the JP material. The difference may be a result of a variety of parameters:

1. greater ratio of thickness to average grain size
2. greater fraction of intragranular fracture
3. finer grain size
4. difference in grain boundary composition and/or structure.

Further work would be necessary to select among these factors.

CONCLUSIONS

1. It is possible to construct a device that will propagate a crack through a thin slab of ceramic and to simultaneously observe the path of the crack and the change in force associated with the crack.

2. Cracks are momentarily locked by microstructural features as they proceed through a specimen. These features include grain boundaries and other unknown features.

3. The locking of cracks at grain boundaries does not appear to be explainable on the basis of direction change alone. Some additional locking mechanism, such as crack blunting, appears necessary.

4. Cracks traveling through large-grain, polycrystalline ceramics likewise show repeated start-stop behavior, apparently very similar to that observed in bicrystals.

RECOMMENDATIONS FOR FUTURE WORK

1. Some additional refinements are necessary in the crack propagation devices, particular in the area of improvement of available

time-constant. These improvements should take the form of dry, clean conditions for the final assembly of the devices, to reduce the atmospheric drift effect.

2. Studies involving material variables would be best accomplished on very coarse grain (G.S. $\geq$ 200 μ), with appropriate grain-boundary doping or bicrystals containing grain boundary additions of the type being used for deformation studies by Palmour.[16]

ACKNOWLEDGMENT

The author expresses his thanks to Bernard F. Hart for technical assistance during the course of the program.

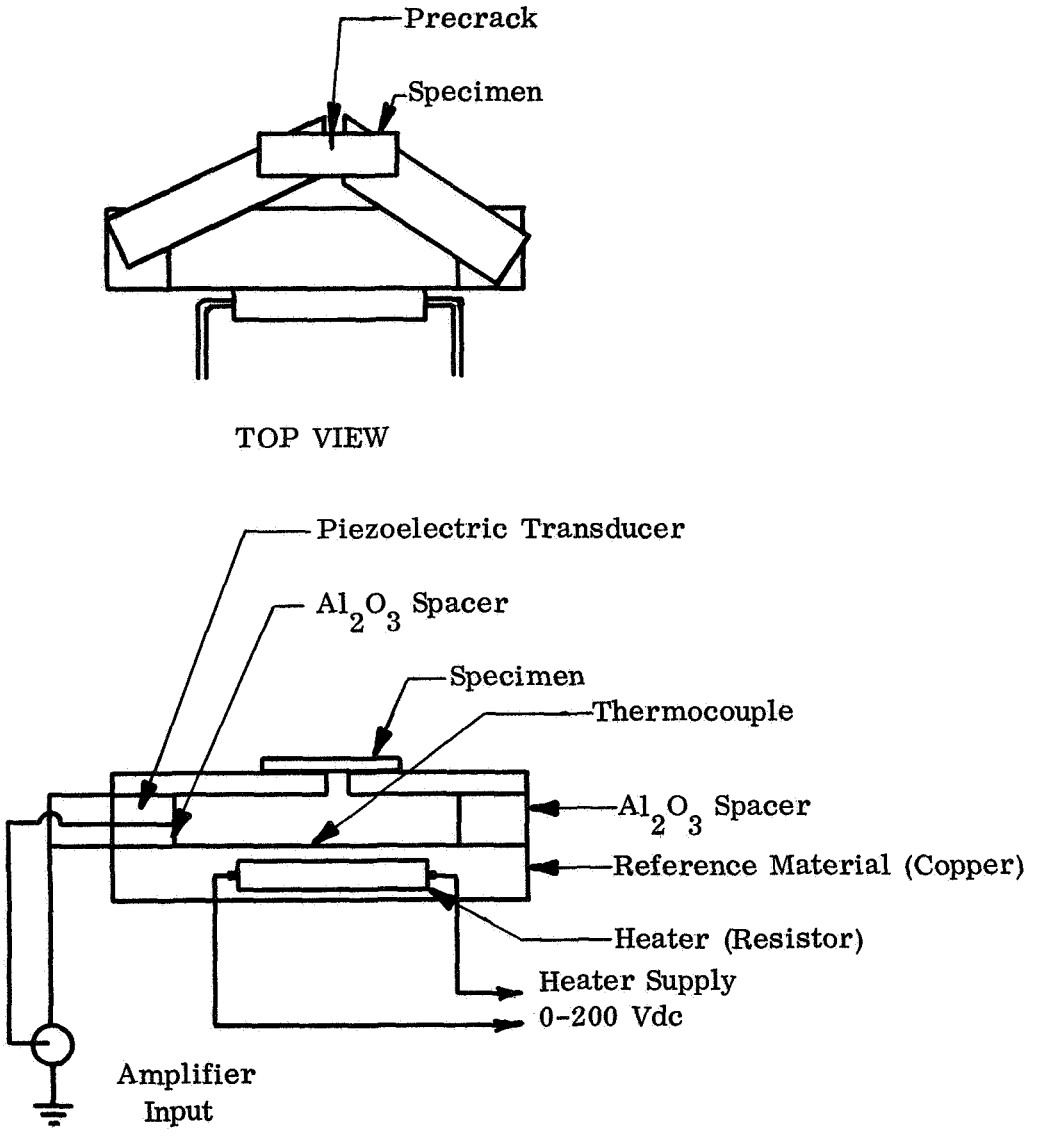

Fig. 1 Strain application device activated by thermal expansion with transducer (shown two times actual size).

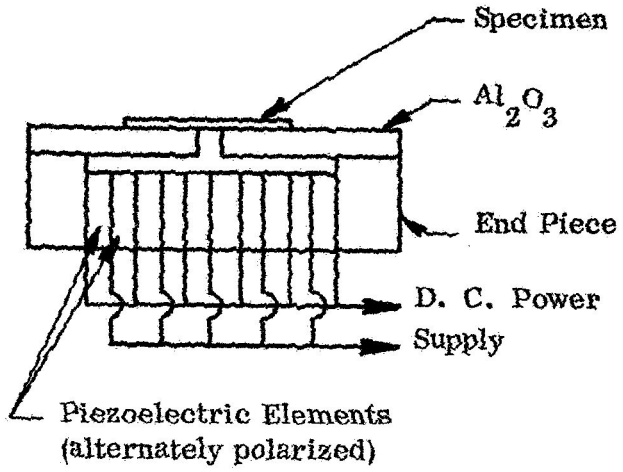

Fig. 2 Strain application device activated by piezoelectric effect (shown two times actual size).

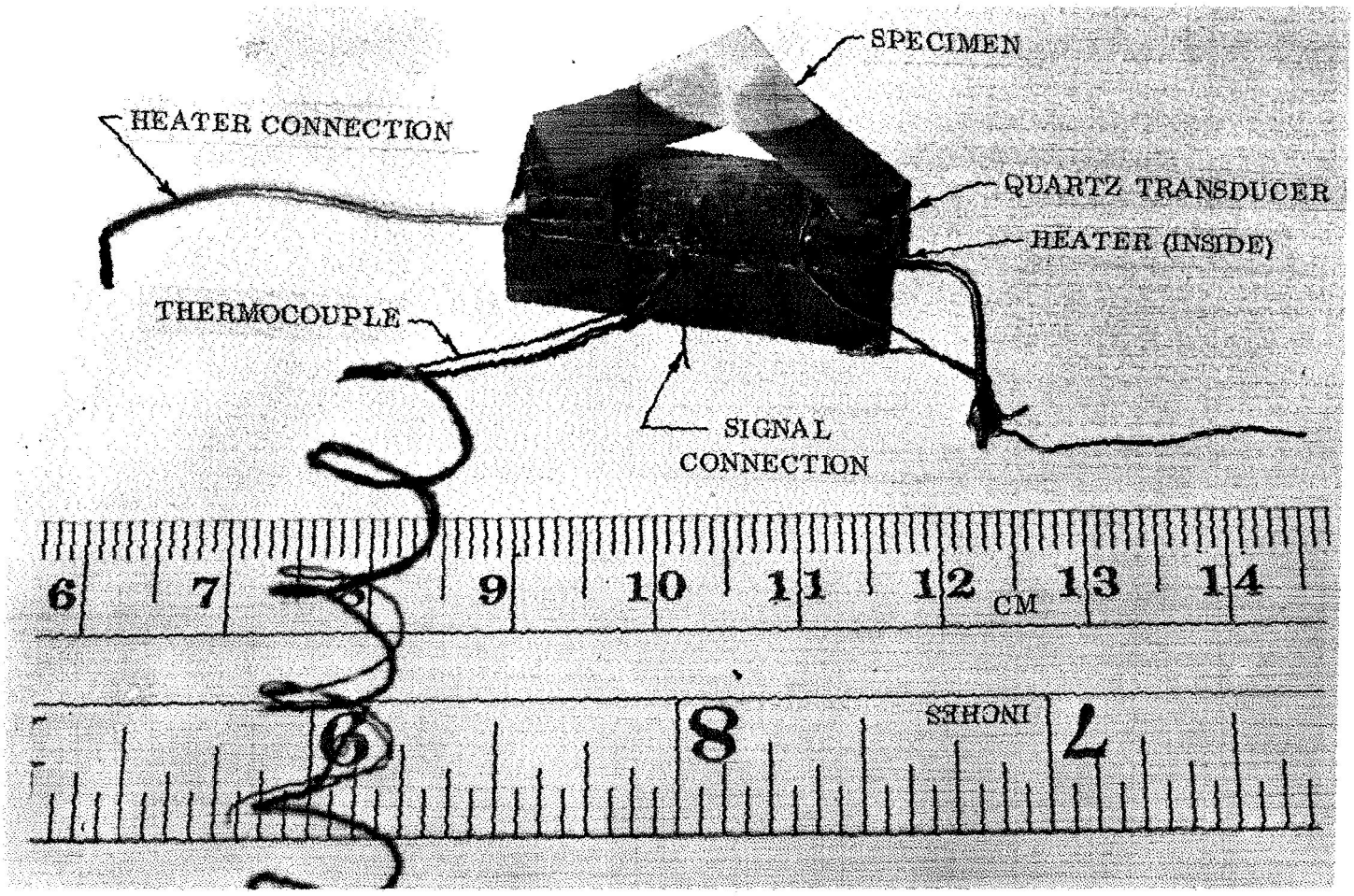

Fig. 3 Final Configuration of Crack Propagation Device

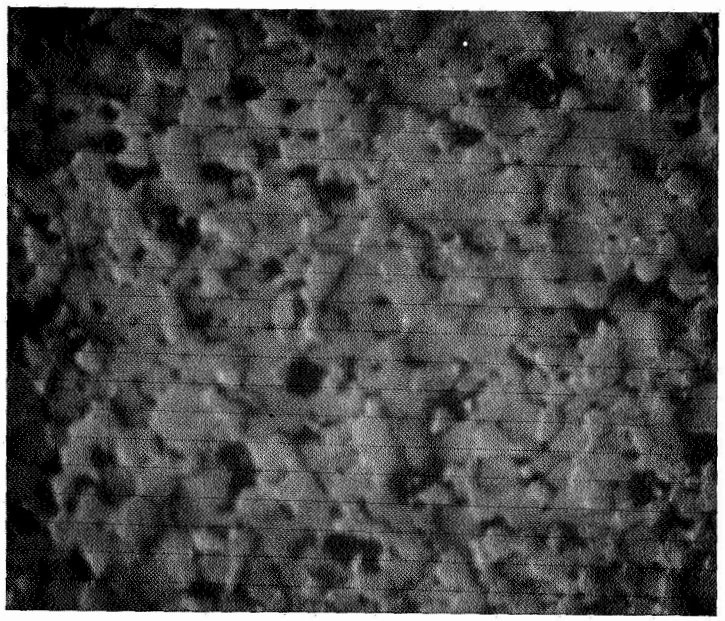

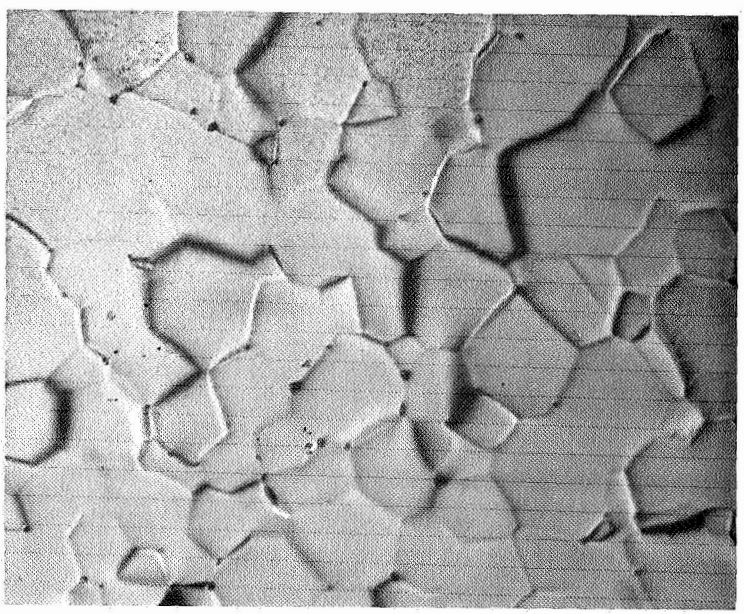

Fig. 4 Typical microstructure of polycrystalline MgO.

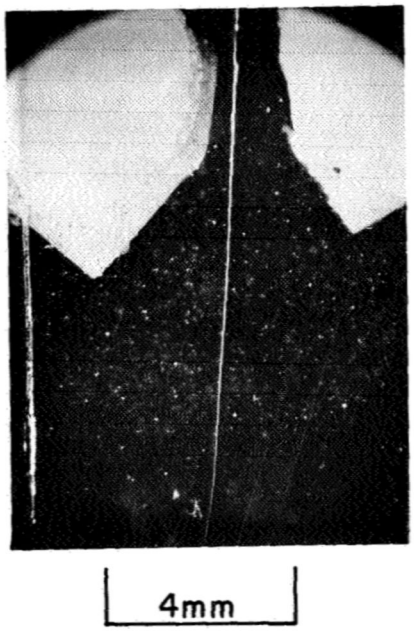

Fig. 5 Glass cover slip after fracture.

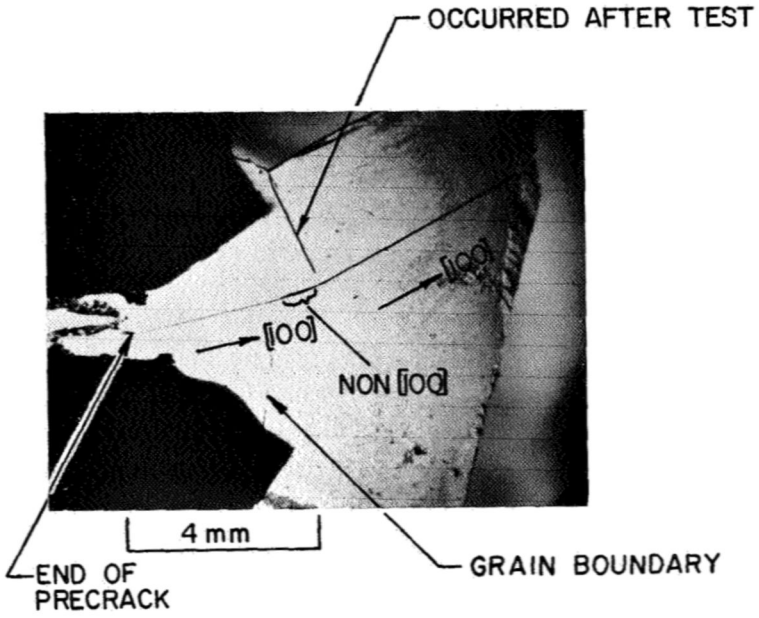

Fig. 6 Norton bicrystal, tilt = 15°, twist = 25° (EST) thickness = 0.15 mm.

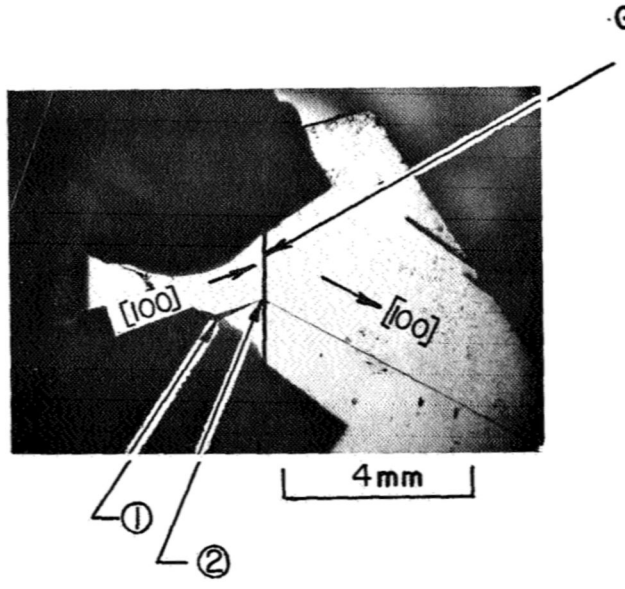

Fig. 7 Norton Bicrystal, tilt = 30°, twist = 30° (est); thickness = 0.17 mm.

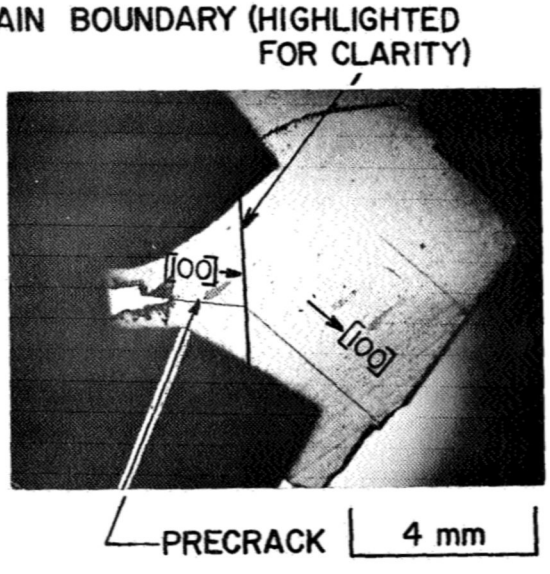

Fig. 8 Norton bicrystal, tilt = 35°, twist = < 10° (EST), thickness = 0.13 mm.

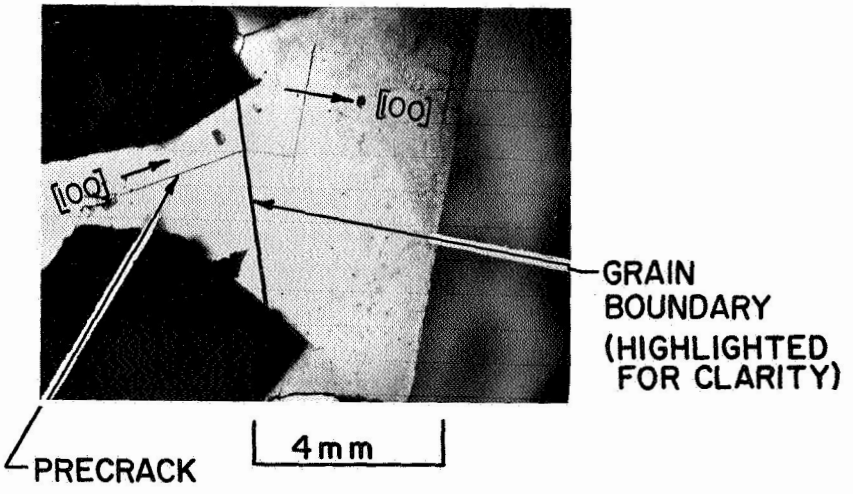

Fig. 9 Norton Bicrystal, tilt = 32°, twist = <10°; thickness = 0.15 mm.

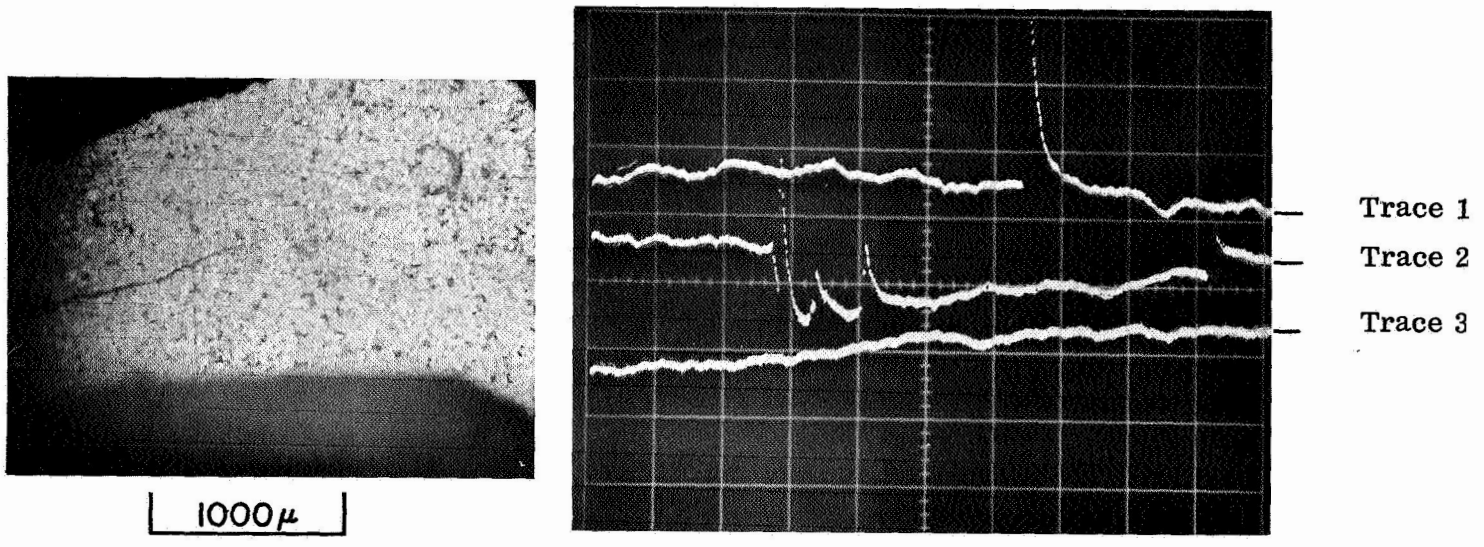

a Sample showing precrack (transmitted light)

b Oscilloscope trace
Vertical scale = 0.1 V/div (~0.1 lb/div.)
Horizontal scale = 0.5 sec/div

Fig. 10 JP material (XIV-6). Trace 1 started with first motion of crack (not recorded) and trace 3 stopped with complete fracture. (Last propagation occurred during retrace and is not shown)

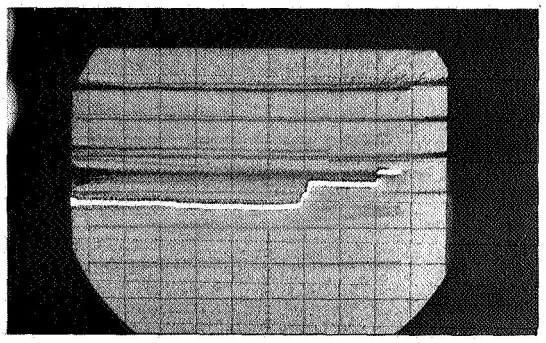

Oscilloscope trace
Vertical scale = 0.5 v/div. (-0.5 lb/div)
Horizontal scale = 0.1 sec/div

Fig. 11 JP material XV-4. (Single trace was self-triggered.)

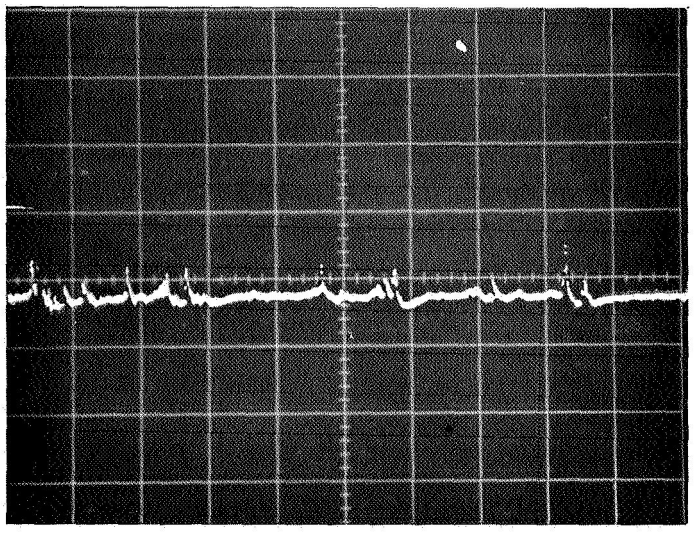

Oscilloscope trace
Vertical scale = 0.1 V/div (0.4 lb/div)
Horizontal scale = 0.5 sec/div

Fig. 12 JF material (single trace triggered at first sign of propagation), time-constant = 0.02 sec.

REFERENCES

1. J. Nakayama, "Direct Measurement of Fracture Energies of Brittle Heterogeneous Materials," J. Am. Ceram. Soc., 48, 583-587 (1965).

2. W. C. Class and E. S. Machlin, "Crack Propagation Method for Measuring Grain Boundary Energies in Brittle Materials," J. Am. Ceram. Soc., 49, 306 (1966).

3. F. P. Knudsen, "Dependence of Mechanical Strength of Brittle Polycrystalline Specimens on Porosity and Grain Size," J. Am. Ceram. Soc., 42, 376-87 (1959).

4. Carniglia, S. C., "Petch Relation in Single-Phase Oxide Ceramics", J. Am. Ceram, Soc., 48, 580-583 (1965).

5. Stokes, R. J., and Li, C. H., "Dislocations and the Tensile Strength of Magnesium Oxide", J. Am. Ceram. Soc., 46, 423-434.

6. B. J. Hockey, "Observation of Plastic Deformation at Microhardness Indentations in Sapphire," Paper 11-13-69 Amer. Cer. Soc., Washington, D. C., 1969.

7. R. C. Ku and T. L. Johnston, "Fracture Strength of MgO Bicrystals," Phil. Mag. 9, 231, (1964).

8. Rice, R. W., and Hunt, J. G., "Identifying Optimum Parameters of Hot Extrusions", Joint Interim Report from the Boeing Company, Space Division, and Whittaker Corporation, Nuclear Metals Division, May 1967. (Available through the National Aeronautics and Space Administration, Office of Scientific and Technical Information, Attn: AFSS-A, Washington, D.C.).

9. R. H. Herron and W. J. Smothers, "Technique for Microscopic Observation of Crack Propagation," American Cer. Soc. Bulletin, 46, 181-185 (1967).

10. F. J. P. Clarke, H. G. Tattersall and G. Tappin, "Toughness of Ceramics and Their Work of Fracture," Proc. Brit. Ceram. Soc. 6, 163-173 (1966).

11. J. J. Gilman, "Direct Measurements of the Surface Energies of Crystals," J. Appl. Phys. 31, 2208-2218 (1960).

12. Nielsen, T. H., and Leipold, M. H., "Hot-Pressed High-Purity Polycrystalline MgO", Bull. Am. Ceram. Soc., 45, 281-285 (1966).

13. M. L. Van Dresser, "Development with High Purity Periclase", Amer. Cer. Soc., Bull. 46, 197 (1967).

14. S. M. Wiederhorn, A. M. Shorb and R. L. Moses, "A Critical Analysis of the Theory of the Double Cantilever Method of Measuring Fracture Surface Energies," J. Appl. Phys., 39, 1569-72 (1968).

15. M. Gell and E. Smith, "The Propagation of Cracks through Grain Boundaries in Polycrystalline 3% Silicon-Iron", Acta Met., 15, 253, (1967).

16. H. Palmour III, et. al., "Grain Boundary Sliding in Alumina Bicrystals", Progress Report ORO-3328-9 to U.S.A.E.C. under Contract AT-(40-1)-3328, Dec. 1968.

For copies of publication or for other information address:

Office of Research and Engineering Services
Publication Services
College of Engineering
University of Kentucky
Lexington, Kentucky 40506